Pergamon

Geochimica et Cosmochimica Acta, Vol. 65, No. 1, pp. 95–109, 2001

0016-7037/01 $20.00 + .00

PII S0016-7037(00)00511-1

Reaction of forest floor organic matter at goethite, birnessite and smectite surfaces

JON CHOROVER* and MARY KAY AMISTADI

Soil Science Program, Department of Agronomy, 116 ASI Building, The Pennsylvania State University, University Park, PA 16802-3504 USA

(*Received January* 10, 2000; *accepted in revised form July* 12, 2000)

Abstract—Experiments were conducted to compare the affinity and reactivity of three different minerals for natural organic matter (NOM) in forest floor leachate (FFL) from hardwood and pine forests. The FFLs were acidic (pH 4) with ionic strengths of 1.4 mM (hardwood) and 1.1 mM (pine), and they contained larger organic molecules (weight average molecular weights [Mw] = 5–6 kDa) than has been reported recently for surface waters using similar methods. A synthetic diluent solution was prepared to match the inorganic chemistry of the FFL and to provide a range of initial dissolved organic carbon (DOC) concentrations (0–140 g C m^{-3}) for reaction with goethite (α-FeOOH), birnessite (δ-MnO_2) and smectite (montmorillonite, SWy-2) in suspension, and in corresponding blanks.

A variety of macroscopic and spectroscopic methods were employed to show that reaction with the three minerals resulted in distinctly different NOM adsorption, fractionation and transformation patterns. Goethite exhibited a steep initial slope in the adsorption isotherm and a maximum retention of 10.5 g C kg^{-1}. The isotherm for montmorillonite was more linear, but equal amounts of C were adsorbed to goethite and montmorillonite (per unit sorbent mass) at maximum DOC. Whereas preferential uptake of high Mw, aromatic constituents via ligand exchange was observed for goethite, compounds of lower than average Mw were retained on montmorillonite and no preference for aromatic moieties was observed. Birnessite, which has an isoelectric point of pH < 2, retained low amounts of organic C (<2 g C kg^{-1}) but exhibited the highest propensity for oxidative transformation of the NOM. The data indicate that fractionation behavior of NOM is dependent on mineral surface chemistry in addition to sorbent affinity for organic C. This work also emphasizes the fact that abiotic transformation reactions must be considered in studies of NOM interaction with Fe(III) and Mn(IV) containing solid phases. *Copyright © 2001 Elsevier Science Ltd*

1. INTRODUCTION

Dissolved natural organic matter (NOM) release into mineral soils from terrestrial vegetation accounts for 1 to 50 g m^{-2} yr^{-1} of carbon worldwide (Moore, 1997). Mobilization and transport of dissolved NOM result in nutrient export to streams and groundwaters, subsurface migration of metals and colloids, and facilitated transport of organic contaminants (Meyer, 1994; Johnson and Amy, 1995; Schiff et al., 1997). Organic horizons of forest soils are loci of particularly high dissolved organic carbon (DOC) concentrations with values typically ranging from 10 to 100 g C m^{-3} (Currie et al., 1996; Goyne et al., 2000). The NOM entering mineral soils from the forest floor includes low molecular weight organic acids, amino acids, nucleic acids, phenolic compounds, carbohydrates, sugars, fatty acids and associated derivatives (Vance and David, 1991; Guggenberger and Zech, 1994; Wershaw et al., 1996). This NOM is highly reactive and distinct from surface water humic substances, but generalizations regarding its composition are difficult because soil interstitial waters are among the least studied of all NOM environments (Malcolm, 1993; Guggenberger and Zech, 1994). Most of the DOC is removed from solution in the top meter of mineral soil as a result of sorption to mineral surfaces and subsequent biodegradation reactions (McDowell and Wood, 1984; Qualls and Haines, 1991; Herbert and Bertsch, 1995). Mineral-sorbed NOM alters the reactivity of the underlying mineral solids by changing their surface functionality and charge (Tipping and Cooke, 1982; Davis, 1982; Chorover and Sposito, 1995; Chorover et al., 1999), whereas those NOM constituents that remain in solution are transported to surface water and serve as carriers for complexing metals and organics.

Prior work has focused on NOM adsorption to iron and aluminum oxides and hydroxides (Tipping, 1981; Tipping, 1990; Schlautman and Morgan, 1994; Gu et al., 1995; Varadachari et al., 1997). Recent work has shown that fractionation of aquatic (surface water) NOM occurs upon sorption to Fe and Al oxide surfaces and this likely contributes to the large adsorption-desorption hysteresis that is observed (McKnight et al., 1992; Ochs et al., 1994; Gu et al., 1995; Wang et al., 1997; Meier et al., 1999; Van de Weerd et al., 1999). Those NOM fractions possessing higher molecular weight, acidity and aromaticity tend to be preferentially adsorbed (Ochs et al., 1994; Kaiser and Zech, 1997; Wang et al., 1997) through a ligand exchange mechanism (Parfitt et al., 1977; Gu et al., 1995). Chromatographic separation of NOM into hydrophobic and hydrophilic fractions before sorption experiments also indicates higher sorption of the former when results are expressed on a C basis (Gu et al., 1995; Kaiser and Zech, 1997). Conversely, sorption on 2:1 layer-type aluminosilicate surfaces is thought to result from cation bridging, entropy-driven processes and hydrophobic interactions (Clapp et al., 1991; Varadachari et al., 1991; Baham and Sposito, 1994), but associated NOM fractionation patterns are not known. The nature of mineral surfaces present in receiving soils likely impacts the preferential uptake of forest floor-derived NOM constituents, but no comparative studies of a range of inorganic solids present in soil environments have been conducted to date.

*Author to whom correspondence should be addressed (jdc7@psu.edu).

In contrast to sorption studies, redox reactivity of soil minerals and associated NOM transformation reactions have received relatively little attention. Experiments with model organic molecules have shown that Fe(III) and Mn(III or IV) oxides are capable of oxidizing reduced C compounds in abiotic systems (Hering and Stumm, 1990; Suter et al., 1991; Stone et al., 1994) but the heterogeneity of NOM has precluded detailed investigation of its transformation upon reaction with mineral surfaces. Indeed, changes in the composition of NOM solutions after contact with iron oxide surfaces have been attributed solely to fractionation upon adsorption (Gu et al., 1995; Wang et al., 1997; Meier et al., 1999), whereas the potential for redox-induced transformation has not been explored. Furthermore, the interaction of NOM with Mn(IV) oxides (e.g., birnessite) has not been examined in detail; these solids exhibit low overall retention of anionic polyelectrolytes due to strong surface acidity and a low point of zero charge. However, prior work has indicated that Mn(IV) in birnessite can act as an electron acceptor to oxidize model phenolic compounds such as those that occur in NOM (Shindo and Huang, 1982; Stone and Morgan, 1984; McBride, 1989; Majcher et al., 2000). Therefore, despite a relatively low capacity for NOM retention, these redox active mineral phases may alter dissolved NOM through chemical transformation reactions. Similar transformations may also be expected to result from Fe oxide-NOM interactions.

This study was conducted to examine the reaction of forest floor leachate NOM with goethite, birnessite and smectite surfaces under solution chemical conditions comparable to those encountered in forest soils. The primary objectives were (1) to assess the effects of mineral surface chemistry on NOM fractionation; (2) to measure changes in NOM composition resulting from surface-mediated redox reactions; and (3) to determine whether the type of forest floor material (oak or pine) had a significant impact on NOM-mineral interactions.

2. EXPERIMENTAL METHODS

2.1. Extraction and Analysis of Forest Floor Leachate

All extractions and experiments were conducted in the dark to prevent photochemical reactions. Humified organic horizons (Oa) were sampled in hardwood and pine stands at the Harvard Forest (Petersham, MA). The major tree species are white oak (*Quercus rubra* L.) and red pine (*Pinus resinosa* Ait.) in the hardwood and pine stands, respectively. Soils were formed from schistose and gneissic glacial till. Field moist samples were sieved to remove and discard the fraction $>$ 2mm. The sieved material was frozen before use. Leachate samples were generated by extracting 250 g of oven-dry equivalent sieved material for 24 h in 1.0 kg of ultrapure H_2O. Each leachate sample was subjected to centrifugation and filtration to remove particulate matter, microbial biomass and extracellular enzymes, so that abiotic interactions could be studied unambiguously. Forest floor suspensions were centrifuged at 10000 relative centrifugal force (RCF) for 20 min to remove light fraction organic matter, prefiltered through 1 μm Whatman A/E glass fiber filters, centrifuged again at 27000 RCF for 20 min and, finally, ultra-filtered through a 10 kDa Amicon Diaflo (YM 10) membrane in a stirred cell. The ultrafiltrate solutions were used as the starting material in reaction with mineral phases.

Ultrafiltrate solutions were analyzed for pH, electrical conductivity (EC), DOC (by Shimadzu TOC 5000A), cations (atomic absorption/emission [AA/AE] spectrometry and Technicon autoanalyzer for NH_4^+), and inorganic and selected organic anions (ion chromatography [IC] and high performance liquid chromatography [HPLC]). A synthetic leachate ("diluent") was prepared from ACS grade inorganic reagents and ultrapure water (MilliQ UV-plus) to match the inorganic chemistry (ion concentrations, pH, EC) of the FFL as closely as possible, but without NOM. Chloride concentration was permitted to exceed the measured FFL value to provide charge balance in the absence of DOC. The diluent was used to adjust DOC values of FFL over a range desired for experiments. Functional group acidity of the NOM was measured by alkalimetric titration of leachate, under N_2 gas, from pH 3 to pH 9 (Bartschat et al., 1992). The corresponding diluent solution was used as a titration blank.

2.2. Preparation of Mineral Phases

Three common soil minerals with differing surface reactivity were used in the study: goethite (α-FeOOH), birnessite (MnO_2) and montmorillonite. Goethite was synthesized by addition of KOH to $Fe(NO_3)_3 \cdot 9H_2O$ solution until pH 12, and then aging the suspension for 24 h at 60°C (Atkinson et al., 1967). The solid was washed with 1 mM HCl until all residual NO_3^- was removed. It was then rinsed with MilliQ water until the supernatant solution pH was 4.0. The solid was then freeze-dried. Birnessite was synthesized by adding concentrated HCl to a boiling solution of $KMnO_4$ (McKenzie, 1971). The precipitate was washed repeatedly with 1 mM HCl, rinsed with ultrapure water until the supernatant solution pH was 4.0, and then the solid was freeze-dried. The composition of goethite and birnessite precipitates was confirmed by X-ray diffraction and Fourier transform infrared spectroscopy (FTIR).

Wyoming montmorillonite, SWy-2, was acquired from the Source Clay Minerals Repository, University of Missouri. The <2 μm size fraction was collected by centrifugation and cleaned by repeated washing (1.0 mol/L NaCl/0.001 mol/L HCl solution) and centrifugation cycles until the supernatant solution pH was 3.0. The clay was then washed repeatedly with 0.01 mol/L NaCl solution (no acid added) until the supernatant solution pH was 5.5. The exchangeable cation composition of montmorillonite is highly dependent upon solution chemistry. Therefore, before reaction with oak FFL, montmorillonite was equilibrated three times for 30 min with the oak diluent solution to give an adsorbed cation composition (in $mmol_c\ kg^{-1}$) of Ca^{2+} (340 $\pm$ 23), Mg^{2+} (38.5 $\pm$ 0.8), K^+ (6.75 $\pm$ 0.03) and Al^{3+} (65 $\pm$ 14), as measured by extraction of quadruplicate subsamples in 1.0 mol/L ammonium acetate solution. Specific surfaces areas of goethite, birnessite and montmorillonite (measured by N_2-BET) were 50.1 $\pm$ 0.24, 83.8 $\pm$ 0.7 and 36.4 $\pm$ 0.9 $m^2\ g^{-1}$. Since N_2-BET does not measure the interlayer surface area of montmorillonite, total specific surface of montmorillonite (including interlayer) was measured to be 596 $m^2\ g^{-1}$ by ethylene glycol monoethyl ether adsorption (Carter et al., 1986). Electrophoretic mobilities of the three minerals were measured as a function of pH in 0.01 mol/L KCl solution using a Pen Kem Model 501 Lazer Zee Meter (Pen Kem, Bedford Hills, NY).

2.3. Reaction of Forest Floor Leachate with Mineral Phases

Forest floor leachate from the oak stand was reacted with all three minerals to assess the effects of mineral surface chemistry on fractionation (objective 1) and transformation (objective 2). The effects of forest type (objective 3) were measured using goethite as a common mineral sorbent. Goethite, birnessite or montmorillonite was added to 50 mL PTFE centrifuge tubes. Diluent and then FFL were added to give a series of mineral suspensions with solid concentrations of 5 kg m^{-3} for goethite and birnessite, 2.5 kg m^{-3} for montmorillonite, and total organic C concentrations ranging from 0 to 170 g m^{-3}. Identical sets of samples ("blanks") were prepared without minerals added to provide an accurate measure of initial suspension concentrations and to account for any solution phase reactions that might occur in the absence of mineral surfaces. Reaction vessels were capped immediately with teflon-lined lids, covered with aluminum foil, and placed on an end-over-end shaker. After 17 h reaction time, the reaction tubes and blanks were centrifuged for 20 min at 27000 RCF. Supernatant solutions were aspirated by Pasteur pipette and analyzed immediately for pH, DOC, cations (Ca, Mg, K, Na, NH_4, Al, Fe, Zn, Mn after filtration through 0.2 μm membranes), anions (Cl, SO_4, PO_4) and selected low molecular weight organic acids that are prevalent in soil solutions (formic, acetic, propionic, oxalic, malonic). Concentration differences between suspension supernatant and blank solutions were used to calculate adsorption

and release of solutes. The amount of NOM adsorbed (C basis) was computed as:

$$q_C \frac{DOC_{eq,B} - DOC_{eq,S}}{m_s} \quad (1)$$

where q_C is the surface excess of NOM (g C kg^{-1}), $DOC_{eq,B}$ and $DOC_{eq,S}$ are the equilibrium DOC concentrations in supernatant solutions of corresponding blank (*B*) and mineral suspensions (*S*) after the reaction (g C m^{-3}), and m_S is the suspension concentration of adsorbent (kg m^{-3}).

Pelleted solids were washed for 15 min in diluent solution to remove entrained supernatant solution and then freeze-dried for analysis of sorbed organic matter by diffuse reflectance infrared Fourier transform (DRIFT) spectroscopy. Infrared spectra of sorbed NOM were obtained by subtracting DRIFT spectra of diluent-reacted solids (without NOM) from those of NOM-reacted solids. All DRIFT spectra were obtained at 2 cm^{-1} resolution on a Nicolet Magna 560 spectrometer.

2.4. Measure of Changes in DOM Resulting From Reaction With Mineral Surfaces

To assess fractionation and transformation of dissolved NOM upon reaction with the different mineral phases, each supernatant solution from "blanks" and "reacted" samples was analyzed by UV-Vis (Shimadzu 3101PC) and FTIR (Nicolet Magna 560) spectroscopy. Molar absorptivity of filtered supernatant solution was determined as absorbance at 280 nm normalized by DOC concentration. Transmission FTIR spectra of dissolved NOM were obtained at 2 cm^{-1} resolution after drying supernatant solutions onto IR transmissive ZnSe windows. Molecular weight distributions of NOM were measured by high performance size exclusion chromatography (HPSEC) before and after reaction using the method of Chin et al. (1994). The HPSEC data were collected on a Waters Inc. (Milford, MA) HPLC system equipped with a HEMA Bio 40, 8 $\times$ 300 mm column (Polymer Standards Service, Inc.). Samples were preequilibrated with a mobile phase consisting of 0.1 mol/L NaCl solution buffered at pH 6.8 with 5 mM Na-phosphate and diluted, as necessary, to give ca. 30 g C m^{-3} before injection. Samples of lower equilibrium DOC concentration were run by HPSEC also and the detection limit was 3 g C m^{-3}. Samples (100 μL) were injected for a 17 min run-time at 1 mL min^{-1} flow rate. Weight-average molecular weight (Mw) and number-average molecular weight (Mn) of dissolved NOM were calculated from the chromatogram data using the following equations (Determann, 1969):

$$Mw = \frac{\Sigma n_i M_i}{\Sigma n_i} \quad (2)$$

$$Mn = \frac{\Sigma n_i}{\Sigma n_i / M_i} \quad (3)$$

where n_i is the height of the sample HPSEC curve at the elution time i corresponding to a solute of molecular weight M_i. Elution times for NOM were calibrated using random coil polystyrene sulfonate standards of known molecular weight (1.4, 4.3, 6.8, 16.8, 32.0, 48.6 and 77.4 kDa, Polymer Standards Service, Inc.) and acetone.

3. RESULTS AND DISCUSSION

3.1. Leachate Chemistry

The chemical composition of FFL and corresponding diluent solutions are shown in Table 1. After extraction, leachate pH was 3.9 for oak and 4.1 for pine FFL. Oak FFL exhibited higher concentrations of K, Na, NH_4, Al and SO_4, whereas Ca, Cl, PO_4, NO_3 and DOC were higher in the pine FFL. Charge density of the NOM (C basis) at the experimental pH was calculated in two ways: (1) by dividing inorganic cation minus inorganic anion charge ($mmol_c$ m^{-3}) by DOC (g m^{-3}); and (2) by interpolation of base titrations of FFL solutions. Results of both estimates ("C.B. Charge" and "Tit. Charge," respectively) are shown in Table 1. The oak NOM exhibits a higher total acidity than the pine NOM and also a higher degree of dissociation at pH 4. The DOC and pH values are representative of those measured under the respective Oa horizons at the Harvard Forest field site (Currie et al., 1996).

Molar absorptivity (ε) of the pine NOM is slightly higher than that of the oak (Table 1), but these values are both intermediate in comparison to published values for aquatic NOM. Chin et al. (1994) reported that ε values for fulvic acids and NOM from a variety of aquatic sources ranged from 60 to 500 L mol^{-1} C cm^{-1}. These authors and others (Traina et al., 1990; Peuravuori and Pihlaja, 1997) observed a strong correlation between ε 65 and percent aromaticity as measured by nuclear magnetic resonance (NMR) spectroscopy.

The average molecular size of compounds solubilized directly from forest floor material is larger than that reported for aquatic NOM. Our measured values of molecular weight by HPSEC (Mw and Mn in Table 1) are ca. three times higher than those reported for aquatic NOM with comparable molar absorptivities (Chin et al., 1994; Peuravuori and Pihlaja, 1997; Meier et al., 1999; Pelekani et al., 1999). The molecular weights reported in Table 1 correspond to the major peak in HPSEC chromatograms, which eluted at 8.7 min and contained at least 95% of the integrated chromatogram area. A small peak, eluting at 6.9 min and containing approximately 5% of the total area, was also observed for both oak and pine leachate. Weight and number average molecular weights for this peak are 42.6 $\pm$ 0.5 and 40.4 $\pm$ 0.6 kDa for the oak NOM and 39.5 $\pm$ 0.2 and 34.2 $\pm$ 0.4 kDa for the pine NOM, respectively. The presence of the 6.9 min peak indicates that a very small fraction of NOM in both systems is larger than 10 kDa, which was the cutoff of the ultrafiltration step. However, given the prominence of the later peak (8.7 min), it is clear that most of the NOM was indeed found to correspond to an average molecular weight less than 10 kDa.

3.2. Extent of NOM Sorption

Results are presented for the reaction of goethite, birnessite and montmorillonite with oak-derived NOM, as well as for the reaction of goethite with pine-derived NOM. Electrophoretic mobility measurements in the absence of NOM indicated that the isoelectric points (i.e.p.) for both birnessite and montmorillonite are pH $<$ 2, whereas the i.e.p. for goethite is pH 8.4. Hence, birnessite and montmorillonite are both negatively charged at the pH of FFL (pH 4), whereas the goethite surface is positively charged. Adsorption isotherms for oak and pine derived NOM show that they exhibit similar affinities (C basis) for the goethite surface at equilibrium DOC values less than 40 g m^{-3} (Fig. 1). However, the sorption maximum for pine NOM (9 g C kg^{-1} or 0.18 mg C m^{-2}) is lower than that for oak NOM (11 g C kg^{-1} or 0.22 mg C m^{-2}). This may result from the lower charge density of the pine NOM at pH 4 (Table 1). In both cases, maximum sorption was achieved at an equilibrium DOC concentration of $<$120 g m^{-3}. These results are comparable in magnitude to prior studies of aquatic NOM adsorption to Fe oxides. Maximum values for sorbed C obtained by reaction of goethite with Great Dismal Swamp and Suwannee River NOM were 0.23 and 0.31 mg C m^{-2}, respectively (Meier

Table 1. Chemical composition of representative leachate and synthetic diluent solutions.

	Oak leachate	Oak diluent	Pine leachate	Pine diluent
		mmol m^{-3}		
Inorganic constituents				
H^+	138 ± 8.6	142 ± 4.7	79.4 ± 5.6	66 ± 5.2
K^+	370 ± 2.6	425 ± 4.2	179 ± 6.5	164 ± 0.6
Na^+	93 ± 0.9	97 ± 19.3	45 ± 0.1	52 ± 0.1
Ca^{2+}	57 ± 0.2	51 ± 2.8	107 ± 0.7	112 ± 0.1
Mg^{2+}	34 ± 0.1	33 ± 0.8	27 ± 1.1	29 ± 0.1
NH_4^+	129 ± 0.2	14 ± 2.9	86 ± 3.3	<5
Al	117 ± 3.8	111 ± 5.1	89 ± 4.7	85 ± 3.3
Fe	39 ± 0.9	<1	25 ± 0.8	<1
Mn	2.6 ± 0.1	<1	2.9 ± 0.2	<1
Cl^-	92 ± 3.5	1035 ± 14	141 ± 2.9	764 ± 23
SO_4^{2-}	104 ± 1.4	98 ± 1.2	71 ± 1.3	67 ± 2.1
$H_2PO_4^-$	6 ± 1.2	7 ± 1.3	25 ± 0.4	31 ± 4.5
NO_3^-	45 ± 1.0	28 ± 5.5	15 ± 3.5	24 ± 7.8
Σ zM^{z+} (cation charge)	1340 ± 15	1180 ± 26	974 ± 17	820 ± 11
Σ zA^{z-} (anion charge)[a]	350 ± 5	1260 ± 15	323 ± 5	950 ± 25
Σ zM^{z+} − Σ zA^{z-}	990 ± 11	−80 ± 30	651 ± 18	−130 ± 27
Ionic strength[a]	1431 ± 11	1730 ± 26	1150 ± 11	1350 ± 26
EC (μS cm^{-1})	171 ± 4.2	197 ± 18	111 ± 2.1	164 ± 3.0
Dissolved organic matter				
DOC (g m^{-3})	153 ± 0.3	0.7 ± 0.3	185 ± 0.4	1.1 ± 0.5
C.B. charge[b] ($mmol_c$ g^{-1} C)	6.5 ± 0.10	—	3.5 ± 0.16	—
Tit. charge[c] ($mmol_c$ g^{-1} C)	7.1 ± 0.11	—	4.0 ± 0.1	—
Total acidity[d] ($mmol_c$ g^{-1} C)	15.8 ± 0.25	—	8.9 ± 0.32	—
Mw_0^e (Da)	5021 ± 139	—	5626 ± 183	—
Mn_0^f (Da)	3706 ± 176	—	4808 ± 117	—
ε_0^g (L mol^{-1} C cm^{-1})	264 ± 2.1	—	302 ± 2.7	—

[a] Anion charge derived from DOC not included.
[b] Anion charge of FFL NOM at initial pH of experiment, calculated from charge balance (Σ cation—Σ anion)/[DOC]).
[c] Anion charge of FFL NOM at initial pH of experiment, calculated from alkalimetric titration of leachate and diluent (blank). Assumes 30% dissociation of acidic functional groups at pH 3.
[d] Total acidity of DOM measured by alkalimetric titration.
[e] Weight average molecular weight of FFL NOM measured by HPSEC.
[f] Number average molecular weight of FFL NOM measured by HPSEC.
[g] Molar absorptivity ($A_{280\ nm}$/DOC).

et al., 1999). Gu et al. (1994) reported a maximum of 0.32 mg C m^{-2} for wetland NOM adsorption to hematite.

A comparison of adsorption isotherms for oak NOM (C basis) on the three mineral phases is also presented in Figure 1. Goethite exhibits the highest affinity for NOM, as measured from the steep initial slope of the isotherm. Much less NOM is retained on the birnessite surface. The large difference in NOM sorption between goethite and birnessite is attributed to differences in mineral surface chemistry. The low adsorption of NOM on the strongly acidic birnessite surface may be the result of repulsion of "like" charge (NOM and birnessite are negatively charged at pH 4) and/or low residence time of surface active NOM.

The isotherm shapes for goethite and montmorillonite are distinctly different, but equivalent quantities of C are sorbed at the highest DOC values employed (Fig. 1). For montmorillonite, the isotherm slope becomes linear above 10 g m^{-3} DOC and it appears that maximum adsorption was not achieved. Like birnessite, montmorillonite is negatively charged in the experiment. In this case, however, charge derives from isomorphic substitutions in the clay structure (Sposito, 1984). Adsorption of counterions (446 $mmol_c$ kg^{-1} dominated by Ca^{2+}) likely mediates the retention of NOM through cation and water bridging (Theng and Scharpenseel, 1975; Clapp et al., 1991; Baham and Sposito, 1994). A linear regression on the montmorillonite isotherm data gives a slope of 0.080 ± 0.007 m^{-3} kg^{-1}, which is close to that reported by Baham and Sposito (1994) for sewage sludge NOM sorption on Cd saturated montmorillonite (0.082 ± 0.005 m^{-3} kg^{-1}). Indeed, Ca and Cd exhibit similar affinities for both NOM and montmorillonite (McBride, 1994). Baham and Sposito (1994) found no evidence of NOM penetration of the montmorillonite interlayer because X-ray diffraction patterns were unaffected by the extent of adsorption. Calculation of NOM sorption on the basis of *external* montmorillonite surface area (from N_2 BET data) gives a coverage of 0.3 mg C m^{-2} at the maximum value measured, which is 45% higher than the corresponding maximum value for goethite.

3.3. Anion Exchange Reactions

The effects of NOM surface loading on net adsorption of inorganic anions to the three solids was calculated from the difference between ion concentrations in suspension superna-

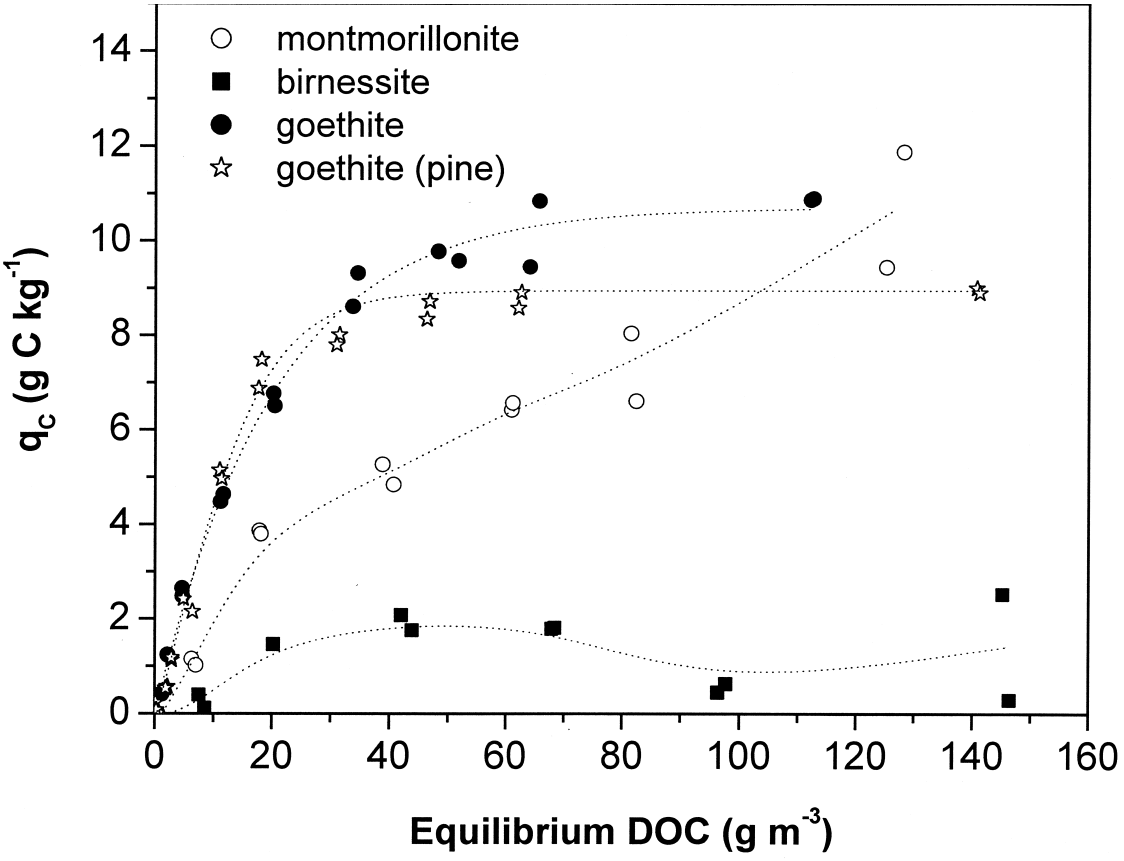

Fig. 1. Adsorption isotherms for FFL NOM on goethite, montmorillonite and birnessite in the dark at pH 4 (C basis). Oak FFL NOM is used for comparison across mineral types, whereas the effect of FFL source (oak versus pine) is assessed using goethite as a common adsorbent.

tant and corresponding blank solutions. For birnessite and goethite, equilibrium pH increased relative to blanks by up to 1.0 and 0.7 pH units, respectively, with increasing NOM adsorption (q_C). No such correlation was observed for montmorillonite. Prior studies with Fe and Al oxides have attributed observed pH increases to displacement of surface hydroxyls during ligand exchange with organic functional groups (Parfitt et al., 1977; Tipping, 1981). Hydroxyl release from goethite increased with increasing adsorption of both oak and pine NOM (Fig. 2a), but the slope of the curve is slightly smaller for the less acidic pine NOM. The slope of the oak NOM function decreases from 8.9 to 1.1 mmol$_c$ g^{-1} C as q_C increases from low (0–2 g C kg^{-1}) to high (4.5–11 g C kg^{-1}) levels. The apparent decreased dependency on q_C may reflect either a diminishing ratio of hydroxyl release to C uptake or an increase in the buffering capacity of soluble OM equilibrated with the solid phase at high surface loadings (Fig. 1.)

Despite a lower overall retention of NOM (Fig. 1), the birnessite reaction results in a larger hydroxide release per unit of adsorbed C than is observed for goethite (Fig. 2a). This difference may result from the lower i.e.p. of birnessite. At pH 4, goethite is net positive charged (surface hydroxyl sites $\equiv FeOH^0$ and $\equiv FeOH_2^+$ are predominant) and birnessite is net negative charged (surface sites $\equiv MnO^-$ and $\equiv MnOH^0$ are predominant) such that the following model reactions are applicable:

$$\equiv FeOH_2^+ + R\text{-}COO^- \leftrightarrow \equiv FeOOC\text{-}R + H_2O \quad (4a)$$

$$\equiv FeOH^0 + R\text{-}COO^- \leftrightarrow \equiv FeOOC\text{-}R + OH^- \quad (4b)$$

$$\equiv MnOH^0 + R\text{-}COO^- \leftrightarrow \equiv MnOOC\text{-}R + OH^- \quad (4c)$$

$$\equiv MnO^- + R\text{-}COO^- + H_2O \leftrightarrow \equiv MnOOC\text{-}R + 2OH^- \quad (4d)$$

where R-COO$^-$ represents a dissociated functional group (e.g., carboxylate) of NOM. Thus, unless only reactions 4b and 4c are operative, a greater OH$^-$ release for birnessite is expected for a given q_C, if other factors are constant. The larger hydroxide release observed for the birnessite-NOM reaction may also derive from abiotic oxidation of NOM constituents (e.g., phenols) in the presence of the Mn(IV) surface. For example, reaction of 1,2-dihydroxybenzene with birnessite results in a large pH increase as surface mediated oxidation yields hydroxide ions along with 1,2-benzoquinone (McBride, 1987). As discussed below, this latter explanation is plausible since we have measured significant oxidative transformation of NOM in the presence of birnessite. For montmorillonite, adsorption of NOM did not result in OH$^-$ release, indicating that the contribution of ligand exchange to adsorption on the 2:1 layer type silicate is relatively small.

Total suspension sulfate concentration was conserved in mixing synthetic diluent and leachate solutions (Table 1) so

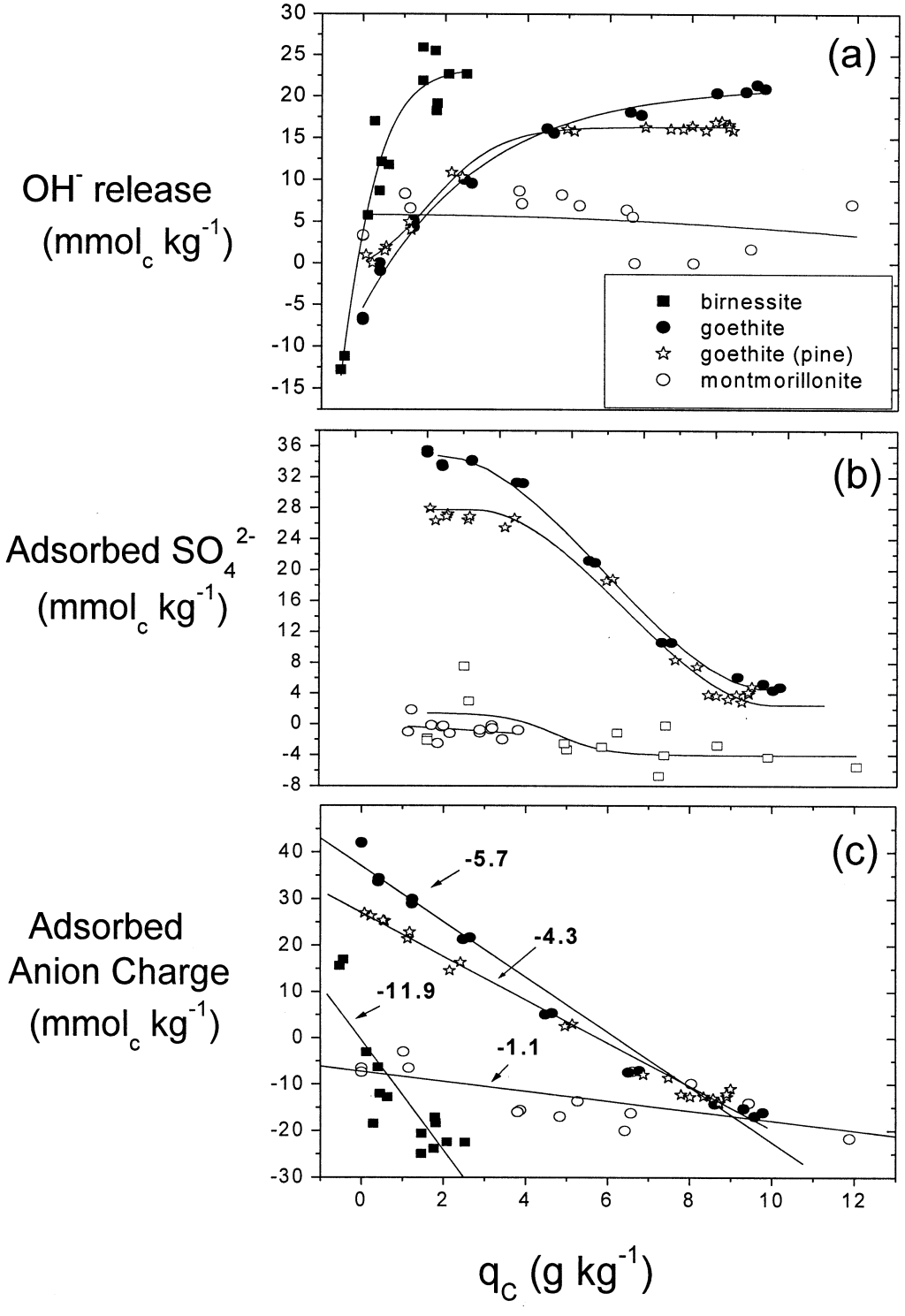

Fig. 2. Anion exchange (millimoles of charge per kilogram of adsorbent) versus quantity of NOM adsorbed (C basis) for the three mineral phases: (a) hydroxyl release, (b) adsorbed SO_4^{2-}, and (c) the sum of net adsorbed inorganic anion charge (OH^- and SO_4^{2-}). Oak FFL NOM is used for comparison across mineral types, whereas the effect of FFL source (oak versus pine) is assessed using goethite as a common adsorbent.

that competition between sulfate and NOM could be evaluated at relevant concentrations. The quantity of SO_4^{2-} adsorbed to the goethite surface is highly dependent on the surface concentration of NOM (q_C). For reaction with oak NOM, adsorbed sulfate decreases from 36 to 4 $mmol_c\ kg^{-1}$ with increasing q_C from 0 to 11 g C kg^{-1} (Fig. 2b). The slightly lower value of adsorbed SO_4^{2-} at a given q_C after reaction with pine FFL is likely a result of the relatively lower concentrations of sulfate

in the contacting solutions (Table 1). The maximum slope of the goethite-oak plot corresponds to an exchange rate of 5.0 $mmol_c\ g^{-1}$ C. Prior work has also indicated competitive adsorption among inorganic ions and organic acids. Gu et al. (1994) found that NOM adsorption to hematite was 30% lower when Na_2SO_4, rather than NaCl, was used as background electrolyte at constant ionic strength (0.01 mol/L). They also reported that increasing NaCl concentration from 0.01 to 0.1 mol/L had no effect on NOM adsorption. Inskeep (1989) reported that SO_4^{2-} adsorption to kaolinite and hydrous Fe oxide was reduced in the presence of organic ligands by an amount that correlated with phenolic and carboxylic content of the ligands. In contrast, since the net charge on montmorillonite and birnessite is negative under the experimental conditions, SO_4^{2-} adsorption to these solid phases is negligible and independent of q_C (Fig. 2b).

For goethite, the total moles of charge resulting from OH^- release and SO_4^{2-} displacement are comparable, but the maximum slopes for these two curves occur at different levels of NOM adsorption. Most of the hydroxide release occurs in the range $0 < q_C < 3\ g\ kg^{-1}$, whereas adsorbed SO_4^{2-} is only slightly reduced at $q_C < 3\ g\ kg^{-1}$. Maximum SO_4^{2-} displacement occurs in the range $3 < q_C < 8\ g\ kg^{-1}$. Evidently, NOM displaces OH^- even at low DOC, but effective competition with SO_4^{2-} requires higher DOC concentrations. Regression of the sum of OH^- and SO_4^{2-} displacement (charge basis) against q_C indicates a linear relation ($r^2 = 0.97$, $p < 0.0001$) for goethite, as shown in Figure 2c. These regression data suggest a displacement of 5.7 and 4.3 mmol of inorganic anion charge per gram of adsorbed C for oak and pine NOM, respectively. The lower value for pine NOM is consistent with its lower acidity and charge (Table 1). Data for birnessite in Figure 2c are dominated by the large hydroxide release and are less well correlated with q_C ($r^2 = 0.71$, $p < 0.001$), suggesting that factors other than NOM adsorption may contribute to the observed pH increase. The relationship of adsorbed anion charge to q_C is weakest for montmorillonite (Fig. 2c, $r^2 = 0.45$, $p < 0.01$). Although ligand exchange on edge aluminol groups may contribute to overall adsorption of NOM on montmorillonite, its contribution appears to be small since adsorbed anion charge is not sensitive to changes in q_C. This is consistent with prior studies that indicate that dissociated humic functional groups are bound to exchangeable cations on the basal surface (Theng, 1979). Although humic acid hydrophobicity may also contribute to its adsorption (Nayak et al., 1990), this physical interaction is not considered to be the dominant mode of association (Varadachari et al., 1994).

3.4. Adsorptive Fractionation

The composition of dissolved NOM after reaction was dependent upon the mineral sorbent. Relative to unreacted NOM (blanks), the major peak (ca. 9 min) in HPSEC chromatograms eluted later after reaction with goethite, earlier after reaction with montmorillonite and at the same time after reaction with birnessite. This corresponds, respectively, to decreasing, increasing and unchanged molecular weight of dissolved NOM. Weight average molecular weight (Mw) for the main peak is plotted as a function of equilibrium DOC in Figure 3a. The shaded areas represent the 95% confidence band of Mw for unreacted pine and oak NOM (blanks) and provide a reference for corresponding reacted samples. The Mw was independent of equilibrium DOC for unreacted samples, as reported for other NOM sources (Wang et al., 1997; Meier et al., 1999).

Goethite effectively removes higher molecular weight material from solution at low equilibrium DOC (Fig. 3a). Fractionation is greatest (Mw of soluble NOM is lowest) where the isotherm slope (Fig. 1) is also greatest and similar results were obtained for pine and oak NOM. As the isotherm begins to level off with increased surface loading of NOM (Fig. 1), the fraction of the total that is adsorbed to the surface is diminished, and changes in Mw relative to unreacted NOM are also reduced. This is clearly shown in Figure 3b where the fraction Mw/Mw_0 is plotted versus the fraction of NOM adsorbed (C basis). The value of Mw_0 is the mean Mw for unreacted NOM from Table 1.

Our data for goethite are consistent with prior studies that have shown preferential adsorption of higher molecular weight NOM constituents on oxides and kaolinite. Davis and Gloor (1981) reported selective uptake of high molecular weight compounds from lake water on alumina. Adsorption of Suwannee River fulvic acid to goethite was likewise associated with the higher Mw fraction (Wang et al., 1997). Meier et al. (1999) observed that adsorption of Suwannee River and Great Dismal Swamp NOM on goethite and kaolinite was accompanied by a reduction in Mw of dissolved NOM. They found that goethite adsorbed more NOM than kaolinite at a given equilibrium DOC concentration and that this resulted in a greater fractionation of NOM. However, their Mw values for both unreacted and reacted aquatic NOM samples were ca. half as large as those reported here. Since these authors used the same HPSEC methods of measurement, there do appear to be significant differences in the molecular size of FFL and aquatic NOM.

This is the first study to report on fractionation of NOM upon adsorption to montmorillonite. In stark contrast to the pattern for goethite, adsorption to montmorillonite is accompanied by a small but significant increase in Mw of dissolved material relative to unreacted NOM ($Mw = 5020 \pm 139$ Da, lower gray band in Fig. 3a), indicating a selective uptake of lower molecular weight material (Fig. 3). To the extent that NOM functionality covaries with molecular weight, differences in Mw fractionation on goethite and montmorillonite are also reflected in spectroscopic data (discussed below). Reaction with birnessite does not significantly affect Mw of NOM (nearly all points for birnessite fall within the confidence band for unreacted oak NOM), which is consistent with low overall adsorption to the Mn oxide surface (Fig. 1). However, it should be noted that the small (<5% of the total area) 43 kDa peak, eluting at 6.7 min, was completely eliminated after reaction with birnessite, whereas it remained in blanks and in NOM solutions resulting from reaction with montmorillonite and goethite (data not shown).

Molar absorptivity (ε) of dissolved NOM (remaining in solution) is significantly reduced after reaction with goethite and (to a lesser extent) birnessite, whereas reaction with montmorillonite does not have an effect on ε (Fig. 4). Except for the lowest equilibrium DOC datum, ε values for montmorillonite-reacted NOM are not significantly different from that of the unreacted oak NOM (lower grey band in Fig. 4a). For goethite, the trend in ε with equilibrium DOC (Fig. 4a) and fractional

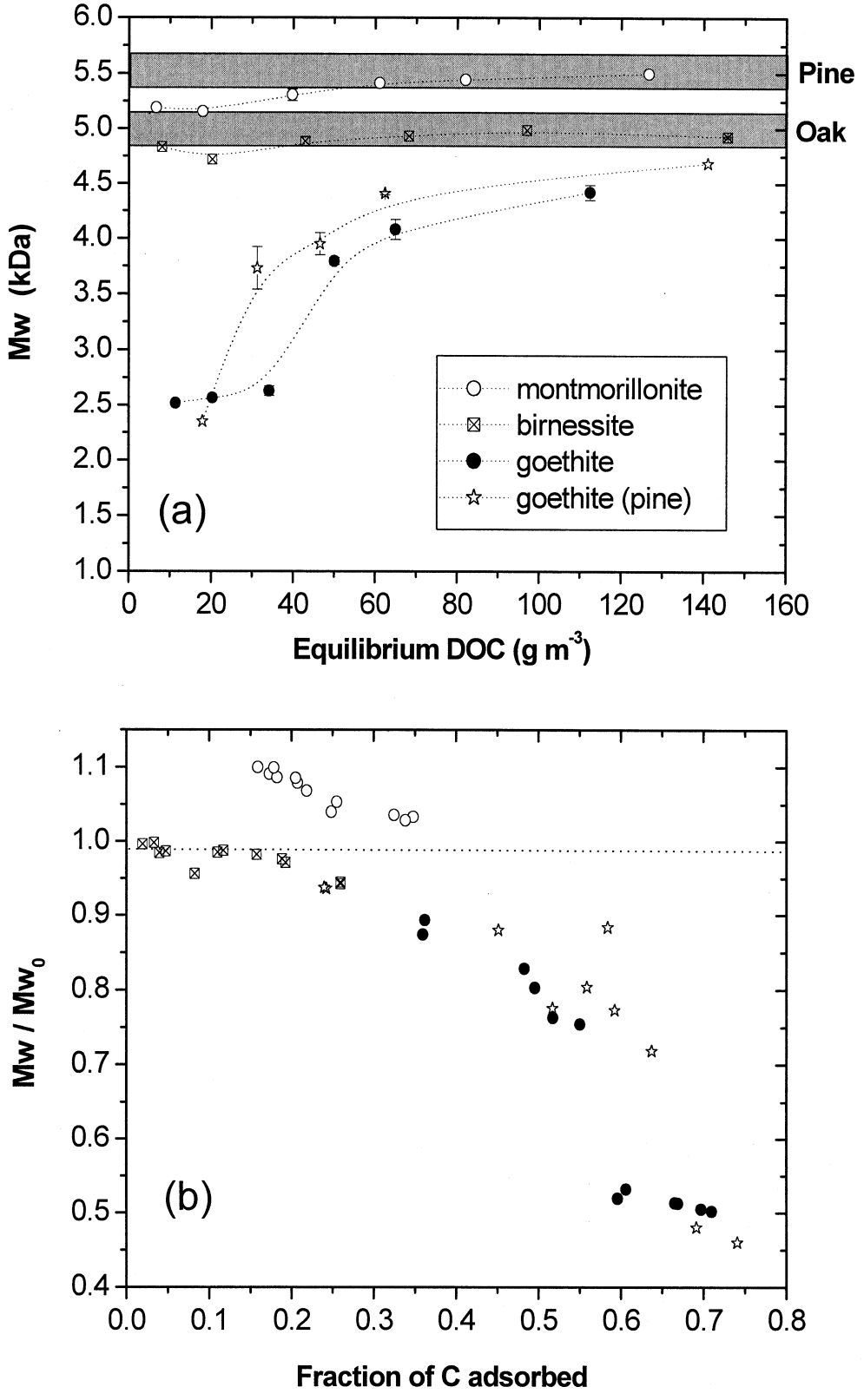

Fig. 3. Effects of reaction with mineral surfaces on weight average molecular weight (Mw) of dissolved NOM as measured by HPSEC. (a) Mw (kilodaltons) versus equilibrium DOC. Grey bands represent the mean ± 95% confidence interval for Mw of unreacted oak or pine NOM, (Mw_0, Table 1). (b) Effects of fractional uptake of organic C (x-axis) on ratio of Mw to mean value for unreacted NOM (Mw_0). Oak FFL NOM is used for comparison across mineral types, whereas the effect of FFL source (oak versus pine) is assessed using goethite as a common adsorbent.

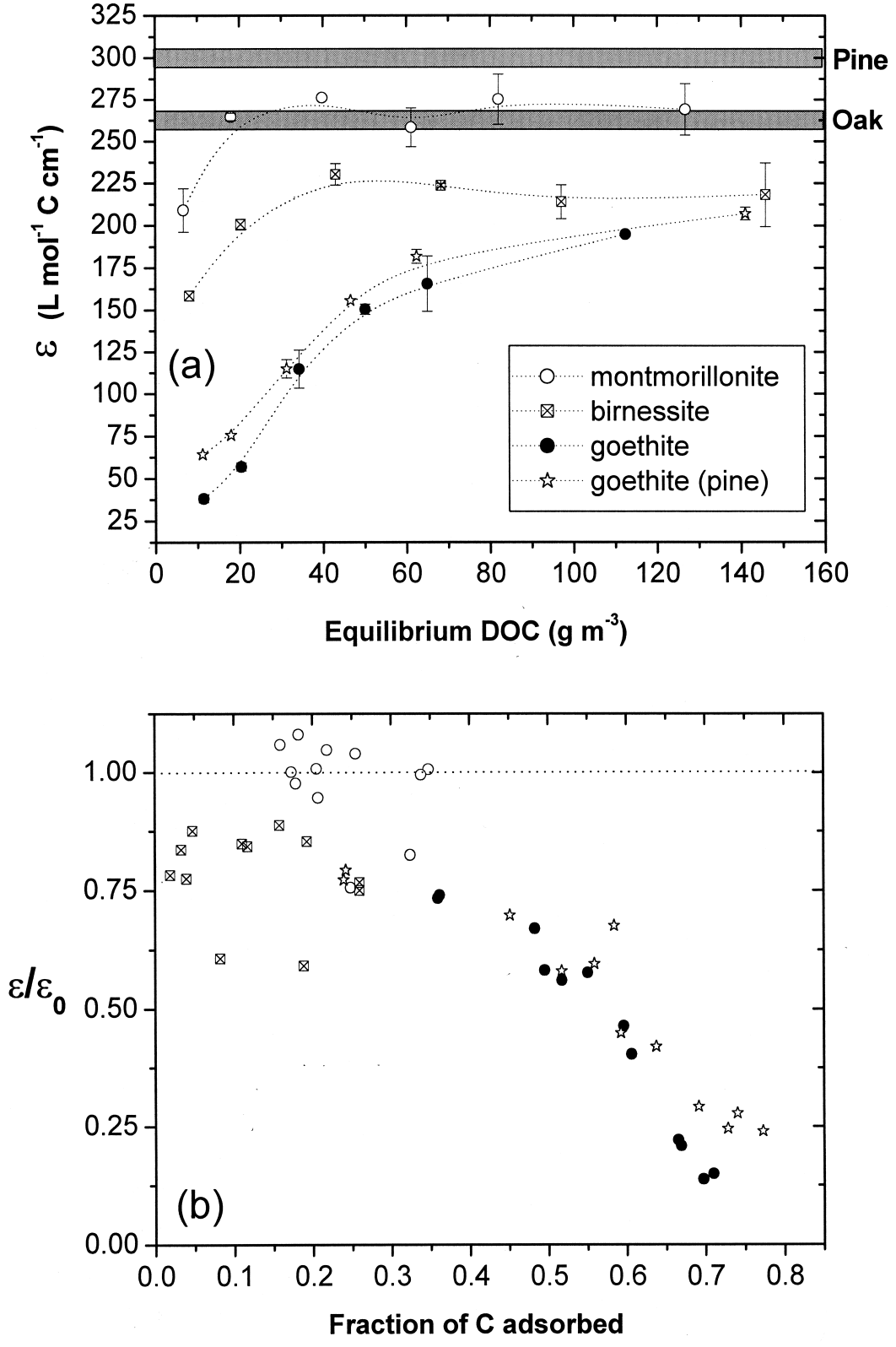

Fig. 4. Effects of reaction with mineral surfaces on molar absorptivity (ε) of dissolved NOM as measured by UV absorbance (280 nm) normalized by DOC. (a) ε versus equilibrium DOC. Grey bands represent the mean $\pm$ 95% confidence interval for ε of unreacted oak or pine NOM (ε_0, Table 1). (b) Effects of fractional uptake of organic C (x-axis) on ratio of ε to mean value for unreacted NOM (ε_0). Oak FFL NOM is used for comparison across mineral types, whereas the effect of FFL source (oak versus pine) is assessed using goethite as a common adsorbent.

uptake (Fig. 4b) mirror those observed for Mw (Fig. 3). Meier et al. (1999) also observed a correlation between Mw and ε and similar trending upon reaction with goethite and kaolinite. The fractional decrease in molar absorptivity with increasing adsorbed fraction of NOM (Fig. 4b) is even greater than that observed for Mw. Conversely, aromatic constituents are not selectively adsorbed to the montmorillonite surface, but rather appear to adsorb in direct proportion to their presence in the bulk NOM solution. These results suggest that the higher Mw NOM is enriched in aromatic moieties. After NOM was reacted with birnessite, molar absorptivity was significantly reduced despite low overall adsorption. These results may reflect a very high selectivity of the birnessite surface for aromatic moieties (despite low overall retention of NOM) or decreased ε may be the result of chemical transformation, possibly including ring cleavage of the NOM as suggested by the extent of hydroxyl release (Fig. 2). Majcher et al. (2000) found that reaction of birnessite with dihydroxybenzene (catechol) at pH 4 resulted in ring cleavage, liberation of CO_2 from the aromatic ring and increased pH. As discussed below, analyses of surface-bound and solution-phase NOM indicate that uptake of aromatic constituents and oxidative transformations both occur during the reaction of NOM with birnessite.

3.5. Infrared Spectroscopy of Reaction Products

Transmission FTIR spectra of oak NOM solutions from unreacted blanks (dashed) and reacted suspensions (solid), are shown in Figure 5. Infrared data pertaining to the pine NOM before and after reaction with goethite were very similar to that of the oak NOM and are not included. The goethite and montmorillonite spectra both show that carboxyl group absorbance bands [$-C=O$ stretch of $-COOH$ is a shoulder at 1720 cm^{-1}, asymmetric $-COO^-$ stretch at 1650 to 1600 cm^{-1}, symmetric $-COO^-$ stretch at 1410 to 1400 cm^{-1}] are diminished relative to carbohydrate and aliphatic components [-C-OH and -C-C- stretching at 1080 to 1040 cm^{-1}] after reaction with mineral surfaces. Both minerals exhibit a preferential adsorption of carboxylic functional groups and the goethite spectra clearly indicate a lower affinity for carbohydrate and/or aliphatic NOM. The 1550 cm^{-1} peak (aromatic C=C stretch) is diminished in all reacted NOM spectra, consistent with the reduction in molar absorptivity discussed above.

Differential diffuse reflectance Fourier transform infrared (DRIFT) spectra of adsorbed NOM are shown in Figure 6. These "difference" spectra are the result of subtracting DRIFT spectra of the unreacted minerals from those of NOM-mineral complexes. The spectra show the prevalence of carboxylate groups on the mineral surfaces, but also reflect mineral-specific differences in the contribution of these groups to the adsorption mechanism. For goethite, loss of carboxyl from solution (Fig. 5a) gives rise to large peaks at 1590 and 1390 cm^{-1} on the surface (Fig. 6a). These peaks correspond, respectively, to asymmetric and symmetric stretching of -COO^- (Baes and Bloom, 1989). The shift in the asymmetric carboxylate stretching band from 1650 cm^{-1} (Fig. 5a) to 1590 cm^{-1} (Fig. 6a) is indicative of the formation of stable Fe-carboxylate complexes on the goethite surface (Gu et al., 1995), as is the emergence of the large peak at 1390 cm^{-1} (Parfitt et al., 1977). These data are consistent with the fact that for goethite, carboxyl group uptake is accompanied by surface OH^- and SO_4^{2-} displacement (i.e., ligand exchange, Fig. 2, whereas no such effect was observed for montmorillonite.

For montmorillonite, removal of carboxylic moieties from solution (Fig. 5b) does not result in a shift in the asymmetric -COO^- stretching band to lower wavenumber upon adsorption (Fig. 6b). Rather, the peak remains at 1650 cm^{-1}, suggestive of a weaker association between -COO^- and hydrated surface cations (Ca^{2+}, Mg^{2+} and K^+) on the layer silicate. Furthermore, peaks at 1170 and 1110 cm^{-1} in the montmorillonite DRIFT spectrum correspond to -C-OH and -C-C- stretching of carbohydrate and aliphatic constituents (Baes and Bloom, 1989; Silverstein et al., 1991). Evidently, the layer silicate surface exhibits a higher affinity than goethite for carbohydrate and aliphatic NOM. This is in agreement with the data on molar absorptivity (Fig. 4) and, in conjunction with the selective uptake of lower Mw NOM (Fig. 3), it suggests that the Mw for this fraction of NOM is lower than for aromatic material. The affinity of smectite for alkyl structures is supported by spectroscopic studies that have shown a concentration of aliphatic organic matter in the fine clay fraction of smectitic soils (Skjemstad et al., 1986; Ristori et al., 1992). However, the uptake of aromatic moieties on all three of the mineral surfaces is evidenced by the loss of the 1550 cm^{-1} peaks (Cothup et al., 1990) in Figure 5 and their appearance in the DRIFT spectra (Fig. 6).

Despite low adsorption (Fig. 1), interaction of NOM with birnessite gives rise to significant and reproducible changes in its transmission FTIR spectrum (Fig. 5b). In particular, there is an increase in the $-C=O$ stretch of $-COOH$ (1740 cm^{-1}), indicating an increase in protonated carboxyl groups in solution, despite an increase in pH. This can be explained by the net production of weakly acidic carboxylic acids upon NOM reaction with birnessite, as was observed using independent chromatographic methods (see section 3.6). There is also a shift (from 1650–1600 cm^{-1}) and an increase in intensity of the asymmetric -COO^- stretching band, in addition to emergence of a strong peak at 1390 cm^{-1} (symmetric $-COO^-$). These results are consistent with the formation of metal-carboxylate complexes, presumably involving Mn released by dissolution as discussed below. The relative decrease in absorbance of aromatic C=C groups (1545 cm^{-1} in Fig. 5b) provides a precise complement to the reduction in molar absorptivity as measured by UV spectroscopy (Fig. 4). This can be explained simply on the basis of adsorption since the DRIFT spectrum for birnessite (Fig. 6) shows peaks corresponding to carboxylate (1650 and 1420 cm^{-1}) and aromatic (1550 cm^{-1}) moieties, in addition to a smaller aliphatic peak (1040 cm^{-1}).

3.6. Transformation Reactions

Prior studies have indicated that Mn(IV) and Fe(III) (hydr)oxides in aqueous suspension can oxidize model phenolic compounds to quinones (McBride, 1987; McBride, 1989), polymerized products (Shindo and Huang, 1982) and/or CO_2 (Majcher et al., 2000). Phenol oxidation is coupled to reductive dissolution of mineral-bound Mn or Fe (Stone and Morgan, 1984; Hering and Stumm, 1990; Suter et al., 1991; Stone et al., 1994). Despite these observations, redox-mediated transformations have rarely been reported in prior studies of NOM-

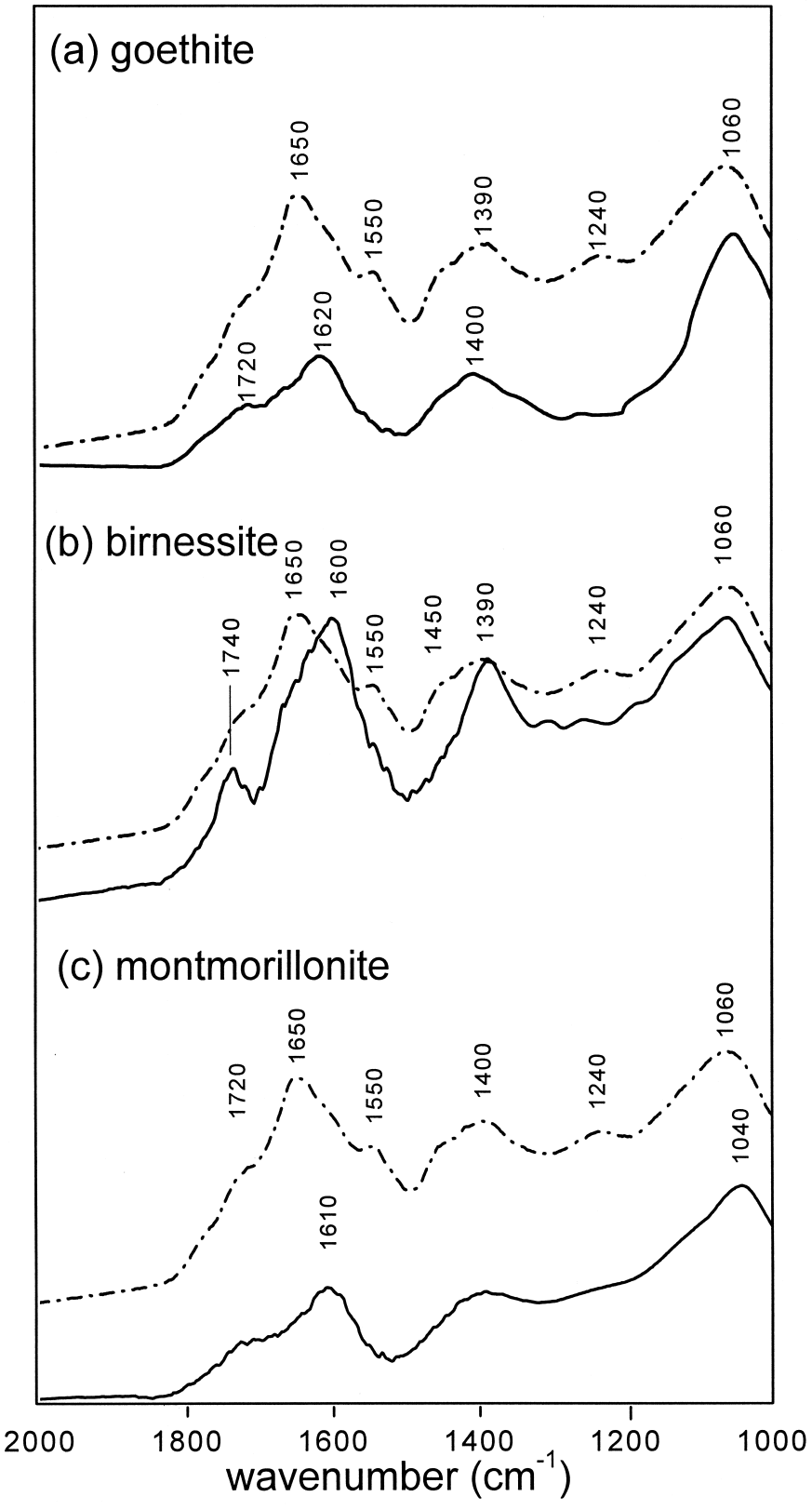

Fig. 5. Transmission Fourier transform infrared spectra of oak FFL NOM in supernatant solutions unreacted (dashed line) and reacted (solid line) with mineral surfaces. Spectra were obtained by drying solutions at 25°C onto infrared transparent (ZnSe) windows: (a) goethite, (b) birnessite and (c) montmorillonite.

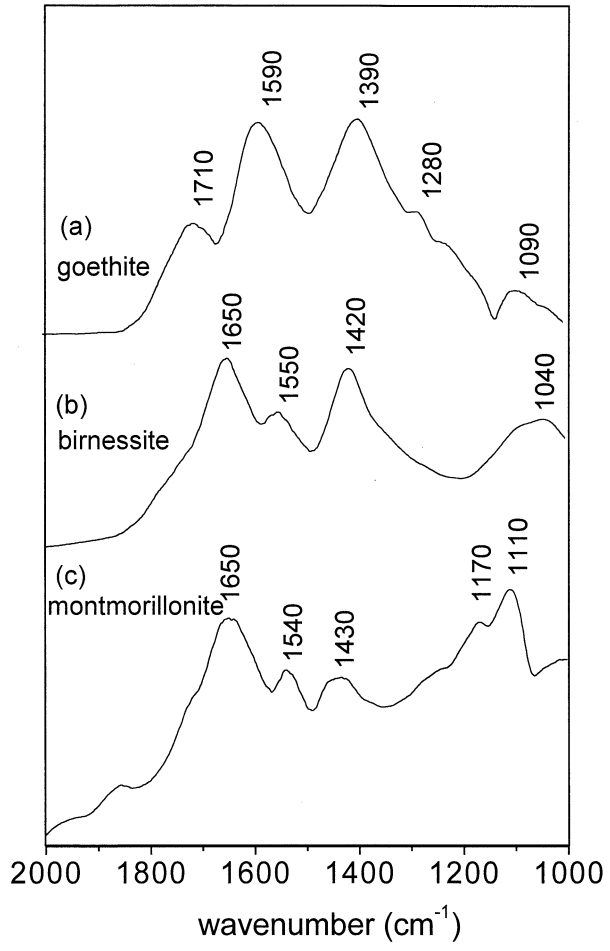

Fig. 6. Differential diffuse reflectance Fourier transform infrared (DRIFT) spectra of oak FFL NOM adsorbed on mineral surfaces. The difference spectra were obtained by subtracting spectra of unreacted minerals from those of the mineral-organic complexes: (a) goethite, (b) birnessite and (c) montmorillonite.

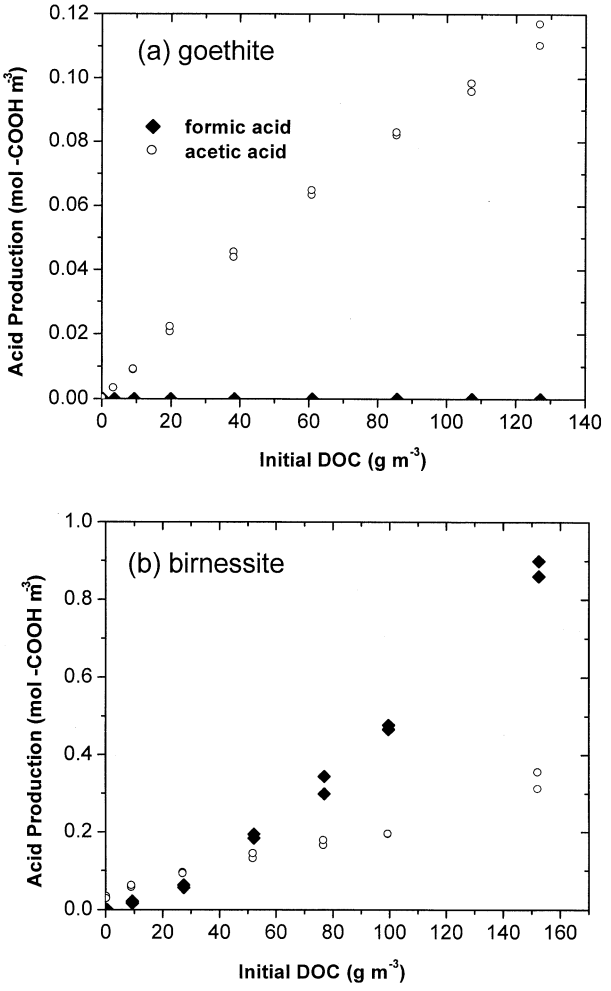

Fig. 7. Concentration of formic and acetic acids in suspension supernatant solutions (oak FFL NOM) after 17 h reaction time in the dark with (a) goethite and (b) birnessite versus initial DOC concentration. Units on the y-axis are moles of carboxylic acid per cubic meter of suspension. These acids were not present at detectable concentrations in the unreacted blanks or in montmorillonite suspensions.

mineral interaction under oxic conditions because of the inherent difficulty of detecting small compositional changes in heterogeneous NOM solutions (Sunda and Kieber, 1994).

Ion chromatography and HPLC were used to measure the composition of low molecular weight organic acids (LMWOA) in oak NOM solutions as affected by reaction with mineral surfaces. Assays were performed specifically for formic, acetic, oxalic, propionic and malonic acids. For blanks (NOM controls with no mineral solids) and for solutions reacted with montmorillonite, ion chromatograms showed no peaks for LMWOA constituents. However, after reaction with goethite and birnessite, new peaks emerged in the chromatograms with retention times corresponding to formic acid (birnessite reaction) and acetic acid (birnessite and goethite reaction) (Fig. 7). Concentrations of these reaction products were well correlated with the amount of DOC added initially to the suspensions. The identities of the peaks were confirmed by analyzing the same samples independently by HPLC with UV detection (Aquasil C_{18} column, 0.05 mol/L phosphate buffer eluent at pH 3). The data in Figure 7 indicate that birnessite more effectively oxidizes the NOM to form LMWOAs. These results are consistent with the transmission FTIR data (Fig. 5b) that show the emergence at 1740 cm^{-1} of the $-C=O$ vibration of $-COOH$. The high reactivity of birnessite may derive from the fact that the reduction of Mn(IV) to Mn(II) occurs at higher redox potentials than does the Fe(III)/Fe(II) reduction (Stumm, 1992). The fact that the birnessite surface is less coated than goethite with adsorbed NOM (Fig. 1) probably also contributes to its enhanced reactivity; it is not as likely to become passivated by NOM blocking of redox active metal sites. Indeed, the low affinity of birnessite for long-term retention of NOM may be key to its high reactivity. The sequence that is generally considered operative in such systems (Stone et al., 1994) involves adsorption of the organic reductant at an (hydr)oxide surface, transfer of electron(s) to the metal center, and subsequent detachment of the reduced metal and oxidized organic. Given that surface complex formation is a prerequisite for mineral catalyzed redox reactions (Suter et al., 1991), the observed oxidative transformation is indicative of adsorption. The parent compounds giving rise to these LMWOAs are unknown but

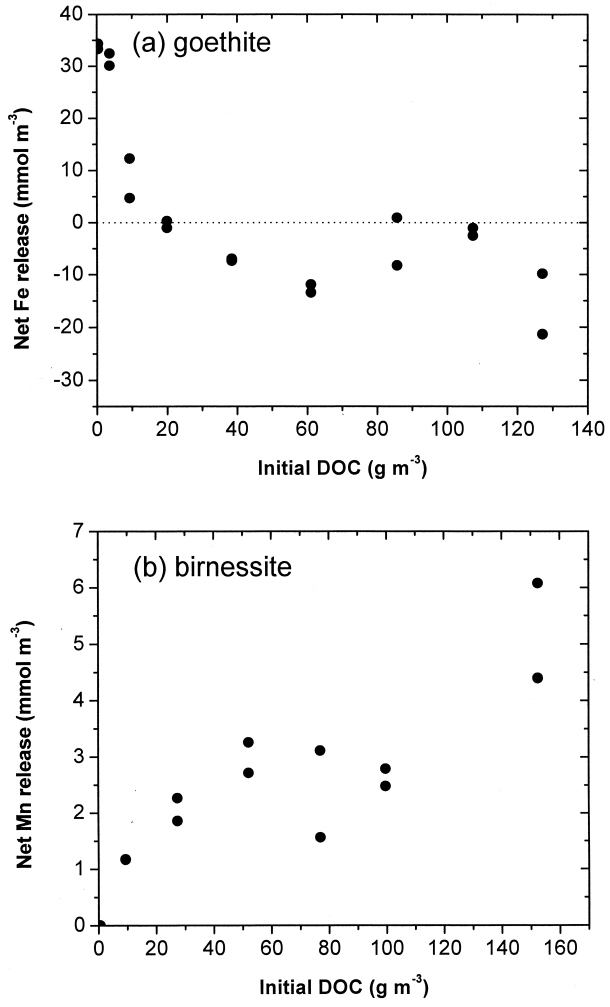

Fig. 8. Net release of Fe and Mn versus initial DOC concentration resulting from reaction of oak FFL NOM with (a) goethite and (b) birnessite.

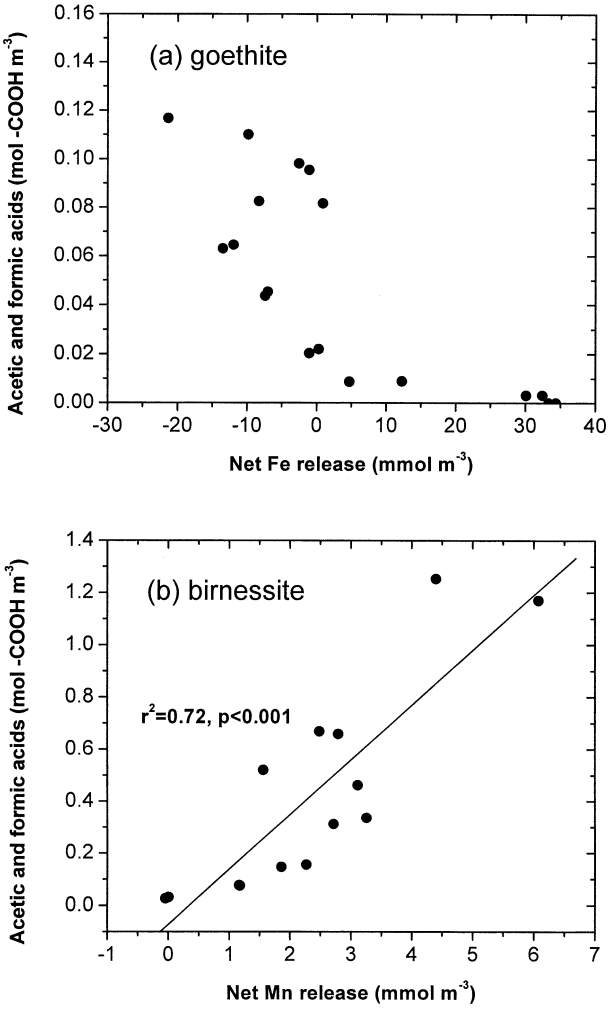

Fig. 9. Relationship between carboxylic acid production from oak FFL NOM-mineral reaction (only acetic and formic acids were detected) and (a) net Fe release from goethite, (b) net Mn release from birnessite.9

may include constituents of lignin and other refractory organic substances whose primary alcohol functionalities can oxidize readily to carboxyl (Clapp and Hayes, 1999).

To couple NOM oxidation to reductive dissolution of birnessite and goethite, the net release to solution of Mn and Fe was calculated from the difference between reacted and blank sample concentrations (Fig. 8). However, this analysis is hindered by the presence of competing reactions. Figure 8a shows that reaction with goethite increased Fe concentration only at low initial DOC concentrations and that supernatant solutions of reacted samples contained less Fe than blanks at [DOC] $>$ 20 g m^{-3}. Several factors likely led to this result. First, both proton and ligand promoted dissolution of Fe from goethite may result in Fe(III) release without reduction of the metal center (Zinder et al., 1986; Stumm, 1992). The negative relationship between Fe release and [DOC] in Figure 8a suggests that proton promoted release of Fe(III) (rather than ligand promoted release or reductive dissolution) was responsible for the positive values at low [DOC]. Second, soluble Fe was present in the oak leachate solutions at a concentration of 40 mmol m^{-3} (Table 1). The decrease to negative values for net Fe release indicates that Fe deriving from the FFL was removed from solution via co-adsorption with NOM to the goethite surface. This suggests that the Fe in FFL is complexed with soluble NOM, which facilitates its surface uptake. Finally, the concentration of Fe in the supernatant solution does not reflect the gross amount of Fe released; once dissolved, it may be readsorbed, complexed with surface-bound NOM, and/or reoxidized. As for the latter, re-oxidation of Fe(II) is faster than Mn(II), even in the presence of catalytic surfaces (Stumm, 1992). As a result of these multiple factors, correlation of acid production with net Fe release was inconclusive (Fig. 9a).

Previous work has indicated that Mn solubilized by reaction of birnessite with phenols is predominantly in the form of Mn(II) (McBride, 1987; McBride, 1989) and that filtration through 0.2 μm nominal pore size filter disks effectively eliminates colloids from subsequent analyses (Stone and Morgan, 1984; Majcher et al., 2000). In contrast to the case for Fe, total Mn concentrations (corrected for [Mn] in blanks) in filtered supernatant solutions were correlated positively with the initial

DOC concentration (Fig. 8b) and, therefore, with the production of acetic and formic acids (Fig. 9b). However, according to the regression in Figure 9b, the molar ratio of acetic plus formic acid to soluble Mn was greater than 200, indicating significant readsorption and/or reoxidation of Mn^{2+} over the 17 h period in oxic suspensions.

4. CONCLUSIONS

Dissolved NOM in oak and pine FFL is of higher molecular weight than that measured recently for aquatic NOM, but charge density, molar absorptivity and functional group composition are similar to materials extracted from surface water. Charge density of FFL NOM from pine forest was lower than from oak. This difference resulted in a lower adsorption maximum and diminished hydroxide release per unit mass of C adsorbed to goethite. Otherwise, FFL NOM extracted from both pine and oak forest floors exhibit similar reactivity with iron oxyhydroxide.

The fractionation and transformation that occurs upon reaction of oak FFL NOM with goethite, birnessite and montmorillonite minerals is dependent on mineral surface chemistry. Positive-charged goethite and negative-charged montmorillonite adsorb comparable amounts of organic C at high equilibrium DOC concentrations, although goethite exhibits a steeper initial isotherm slope. Birnessite was negatively charged at the experimental pH and exhibited low overall retention of NOM. The goethite surface preferentially removes high molecular weight, aromatic compounds from solution and this is accompanied by significant hydroxyl and sulfate displacement. Transmission IR spectra of NOM solutions and differential DRIFT spectra of adsorbed NOM confirm that ligand exchange reactions result in the formation of Fe-carboxylate bonds on the goethite surface. Reaction with montmorillonite results in different fractionation than in the case of goethite. No correlation with hydroxyl release was observed and sulfate sorption was negligible through the range of NOM adsorption. Although IR spectra show surface uptake of carboxylate to the negatively-charged montmorillonite surface, no shift in the carboxylate peak is observed in DRIFT spectra. These results are consistent with a cation or water bridging mechanism. Also in contrast to the Fe oxyhydroxide, adsorption to montmorillonite favors compounds of slightly smaller size than the bulk NOM, and no preferential uptake of aromatic over aliphatic moieties is observed. Although birnessite exhibits low adsorption of NOM, it also shows the highest chemical reactivity, as indicated by production of hydroxide and aliphatic acids. Indeed, the fact that the birnessite surface does not become coated with NOM likely contributes to its proclivity for NOM oxidation.

The results of this study indicate that the extent of adsorption is not itself an adequate predictor of NOM fractionation. In so far as the mechanism of interaction is affected by mineral surface chemistry, so is the nature of the fractionation process. The results also emphasize the potential redox reactivity of oxic mineral-NOM systems. Especially with redox active surfaces such as Fe and Mn (hydr)oxides, chemical transformations are significant and should be considered in future studies.

Acknowledgments—We thank Keith W. Goyne for conducting electrophoretic mobility measurements, K. G. Karthikeyan for EGME surface area measurements, and two anonymous reviewers for constructive comments on the manuscript. Funding was provided by the National Science Foundation Grant no. TECO-9727057.

Associate editor: D. L. Sparks

REFERENCES

Atkinson R. J., Posner A. M., and Quirk, J. P. (1967) Adsorption of potential-determining ions at the ferric oxide-aqueous electrolyte interface. *J. Phys. Chem.* **71,** 550–558.

Baes A. U. and Bloom, P. R.. (1989) Diffuse reflectance and transmission Fourier transform infrared (DRIFT) spectroscopy of humic and fulvic acids. *Soil Sci. Soc. Am. J.* **53,** 695–700.

Baham J. and Sposito G. (1994) Adsorption of dissolved organic carbon extracted from sewage sludge on montmorillonite and kaolinite in the presence of metal ions. *J. Environ. Qual.* **23,** 147–153.

Bartschat B. M., Cabaniss S. E., and Morel F. M. M. (1992) Oligoelectrolyte model for cation binding by humic substances. *Environ. Sci. Technol.* **26,** 284–294.

Carter D. L., Mortland M. M., and Kemper W. D. (1986) Specific surface. In *Methods of Soil Analysis, Part 1-Physical and Mineralogical Methods* (ed. A. Klute), Chap. 16, pp. 413–424. *Soil Sci. Soc. Am.*

Chin Y. P., Aiken G., and O'Loughlin E. (1994) Molecular weight, polydispersity, and spectroscopic properties of aquatic humic substances. *Environ. Sci. Technol.* **28,** 1853–1858.

Chorover J., Amistadi M. K., Burgos W. D., and Hatcher P. G. (1999) Quinoline sorption on kaolinite-humic acid complexes. *Soil Sci. Soc. Am. J.* **63,** 850–857.

Chorover J. and Sposito G. (1995) Surface charge characteristics of kaolinitic tropical soils. *Geochim. Cosmochim. Acta* **59,** 875–884.

Clapp C. E., Harrison R., and Hayes M. H. B. (1991) Interactions between organic macromolecules and soil inorganic colloids and soils. In *Interactions at the Soil Colloid-Soil Solution Interface* (eds. G. H. Bolt et al.), Chap. 12, pp. 409–468. Kluwer.

Clapp C. E. and Hayes M. H. B. (1999) Sizes and shapes of humic substances. *Soil Sci.* **164,** 777–789.

Cothup N. B., Daly L. H., and Wiberley S. E. (1990) Introduction to infrared and Raman spectroscopy. 3rd ed:Academic Press.

Currie W. S., Aber J. D., McDowell W. H., Boone R. D., and Magill A. H. (1996) Vertical transport of dissolved organic C and N under long-term N amendments in pine and hardwood forests. *Biogeochem.* **35,** 471–505.

Davis J. A. (1982) Adsorption of natural dissolved organic matter at the oxide/water interface. *Geochim. Cosmochim. Acta* **46,** 2381–2393.

Davis J. A. and Gloor R. (1981) Adsorption of dissolved organics in lake water by aluminum oxide: Effect of molecular weight. *Environ. Sci. Technol.* **15,** 1223–1229.

Determann H. (1969) Gel Chromatography. Gel Filtration, Gel Permeation, Molecular Sieves. A Laboratory Handbook. [Translated by E. Gross and J. M. Harkin]. Springer-Verlag.

Goyne K. W., Chorover J., and Day R. L. (2000). Artifacts caused by collection of soil solution with passive capillary samplers. *Soil Sci. Soc. Am. J.* **64,** 1330–1336.

Gu B., Schmitt J., Chen Z., Liang L., and McCarthy J. F. (1994) Adsorption and desorption of natural organic matter on iron oxide: Mechanisms and models. *Environ. Sci. Technol.* **28,** 38–46.

Gu B., Schmitt J., Chen Z., Liang L., and McCarthy J. F. (1995) Adsorption and desorption of different organic matter fractions on iron oxide. *Geochim. Cosmochim. Acta* **59,** 219–229.

Guggenberger G. and Zech W. (1994) Dissolved organic carbon in forest floor leachates: Simple degradation products or humic substances? *Sci. Tot. Environ.* **152,** 37–47.

Herbert B. E. and Bertsch P. M. (1995) Characterization of dissolved and collodial organic matter in soil solution: A review. In *Carbon Forms and Functions in Forest Soils* (eds. W. W. McFee and J. M. Kelly), Chap. 5, pp 63–88. *Soil Sci. Soc. Am.*

Inskeep W. P. (1989) Adsorption of sulfate by kaolinite and amorphous iron oxide in the presence of organic ligands. *J. Environ. Qual.* **18,** 379–385.

Hering J. and Stumm W. (1990) Oxidative and reductive dissolution of minerals. In *Rev. Mineral. 23: Mineral-Water Interface Geochemis-*

try, (ed. M. F. Hochella and A. F. White), Vol. 23, pp. 427–465, Mineralogical Society of America.

Johnson W. P. and Amy G. L. (1995) Facilitated transport and enhanced desorption of polycyclic aromatic hydrocarbons by natural organic matter in aquifer sediments. *Environ. Sci. Technol.* **29,** 807–817.

Kaiser K. and Zech W. (1997) Competitive sorption of dissolved organic matter fractions to soils and related mineral phases. *Soil Sci. Soc. Am. J.* **61,** 64–69.

Majcher E. M., Chorover J., Bollag J-.M., and Huang P. M. (2000) Evolution of CO2 during birnessite-induced oxidation of ^{14}C-labeled catechol. *Soil Sci. Soc. Am. J.* **64,** 157–163.

Malcolm R. L. (1993) Concentration and composition of dissolved organic carbon in soils, streams and groundwaters. In *Organic Substances in Soil and Water: Natural Constituents and Their Influences on Contaminant Behaviour* (ed. A. J. Beck et al.), Chap. 2, pp. 19–30. Royal Soc. Chem.

McBride M. B. (1987) Adsorption, oxidation of phenolic compounds by Fe and Mn oxides. *Soil Sci. Soc. Am. J.* **5,** 1466–1472.

McBride M. B. (1989) Oxidation of 1,2- and 1,4-dihydroxybenzene by birnessite in acidic aqueous suspension. *Clays Clay Miner.* **37,** 479–486.

McBride M. B. (1994) The Environmental Chemistry of Soils. Oxford University Press.

McDowell W. H. and Wood T. (1984) Podzolization: Soil processes control dissolved organic carbon concentrations in stream water. *Soil Sci.* **137,** 23–32.

McKenzie R. M. (1971) The synthesis of birnessite, crytomelane, and some other oxides and hyroxides of manganese. *Miner. Mag.* **38,** 493–502.

McKnight D. M., Bencala K. A., Zellweger G. W., Aiken G. R., Feder G. L., and Thorn K. A. (1992) Sorption of dissolved organic carbon by hydrous aluminum and iron oxides occurring at the confluence of Deer Creek with the Snake River, Summit County, Colorado. *Environ. Sci. Technol.* **26,** 1388–1396.

Meier M., Namjesnik-Dejanovic K., Maurice P. A., Chin, Y-.P., and Aiken, G. R. (1999) Fractionation of aquatic natural organic matter upon sorption to goethite and kaolinite. *Chem. Geol.* **157,** 275–284.

Meyer J. L. (1994) The microbial loop in flowing waters. *Microb. Ecol.* **28,** 195–199.

Moore T. R. (1997) Dissolved organic carbon: Sources, sinks, and fluxes and role in the soil carbon cycle. In *Soil Processes and the Carbon Cycle* (eds. R. Lal et al.), Chap. 19, pp. 281–292. CRC Press.

Nayak D. C., Varadachari C., and Ghosh K. (1990) Influence of organic acidic functional groups of humic substances in complexation with clay minerals. *Soil Sci.* **149,** 268–271.

Ochs M., Cosovich B., and Stumm W. (1994) Coordinative and hydrophobic interaction of humic substances with hydrophilic Al_2O_3 and hydrophobic mercury surfaces. *Geochim. Cosmochim. Acta* **58,** 639–650.

Parfitt R. L., Fraser A. R., and Farmer V. C. (1977) Adsorption on hydrous oxides. III. Fulvic and humic acid on goethite, gibbsite and imogolite. *J. Soil Sci.* **28,** 289–296.

Pelekani C., Newcombe G., Snoeyink V. L., Hepplewhite C., Assemi S., and Beckett R. (1999) Characterization of natural organic matter using higher performance size exclusion chromatography. *Environ. Sci. Technol.* **33,** 2807–2813.

Peuravuori J. and Pihlaja K. (1997) Molecular size distribution and spectroscopic properties of aquatic humic substances. *Anal. Chim. Acta* **337,** 133–149.

Ristori G. G., Sparvoli E., de Nobili M., and D'Aqui L. P. (1992) Characterization of organic matter in particle-size fractions of Vertisols. *Geoderma.* **54,** 295–305.

Qualls R. G. and Haines B. L. (1991) Geochemistry of dissolved nutrients in water percolating through a forest ecosystem. *Soil Sci. Soc. Am. J.* **55,** 1112–1123.

Schiff S. L., Aravena R., Trumbore S. E., Hinton M. J., Elgood R., and Dillon P. J. (1997) Export of DOC from forested catchments on the Precambrian Shield of Central Ontario: Clues from ^{13}C and. ^{14}C. *Biogeochem.* **36,** 43–65.

Shindo H. and Huang P. M. (1982) Role of Mn(IV) oxides in abiotic formation of humic substances in the environment. *Nature.* **298,** 363–365.

Schlautman M. A. and J. J. Morgan. (1994) Adsorption of aquatic humic substances on colloidal-size aluminum oxide particles: Influence of solution chemistry. *Geochim. Cosmochim. Acta* **58,** 4293–4303.

Silverstein R. M., Bassler G. C., and Morrill T. C. (1991) Spectrometric Identification of Organic Compounds. John Wiley and Sons.

Skjemstad J. O., Dalal R. C., and Barron P. F. (1986) Spectroscopic investigation of cultivation effects on organic matter of Vertisols. *Soil Sci. Soc. Am. J.* **50,** 354–359.

Sposito G. (1984) The Surface Chemistry of Soils. Oxford.

Stone A. T., Godtfredsen K. L., and Deng B. (1994) Sources and reactivity of reductants encountered in aquatic environments. In *Chemistry of Aquatic Systems: Local and Global Perspectives* (eds. G. Bidoglio and W. Stumm), pp. 337–374. ECSC, EEC, EAEC.

Stone A. T. and Morgan J. J. (1984) Reduction and dissolution of manganese (III) and manganese (IV) oxides by organics: 2. Survey of the reactivity of organics. *Environ. Sci. Technol.* **18,** 617–624.

Stumm W. (1992) Chemistry of the Solid-Water Interface. John Wiley and Sons.

Sunda W. G. and Kieber D. J. (1994) Oxidation of humic substances by manganese oxides yields low molecular weight organic substrates. *Nature.* **367,** 62–64.

Suter D., Banwart S., and Stumm W. (1991) Dissolution of hydrous iron (III) oxides by reductive mechanisms. *Langmuir.* **7,** 809–813.

Theng B. K. G. (1979) Formation and Properties of Clay-Polymer Complexes. Elsevier.

Theng B. K. G. and Scharpenseel H. W. (1975) The adsorption of ^{14}C labeled humic acid by montmorillonite. Proc. Intl. Clay Soc., Mexico City. p. 643–653.

Tipping E. (1981) The adsorption of aquatic humic substances by iron oxides. *Geochim. Cosmochim. Acta* **45,** 191–199.

Tipping E. (1990) Interactions of organic acids with inorganic and organic surfaces. In *Organic Acids in Aquatic Ecosystems.* (eds. E. M. Perdue and E. T. Gjessing), pp. 209–221. John Wiley and Sons.

Tipping E. and Cooke D. (1982) The effects of adsorbed humic substances on the surface charge of goethite (α-FeOOH) in freshwaters. *Geochim. Cosmochim. Acta* **46,** 75–80.

Traina S. J., Novak J., and Smeck N. E. (1990) An ultraviolet absorbance method of estimating the percent aromatic carbon content of humic acids. *J. Environ. Qual.* **19,** 151–153.

Van de Weerd H., van Riemsdijk W. H., and Leijnse A. (1999) Modeling the dynamic adsorption/desorption of a NOM mixture: Effects of physical and chemical heterogeneity. *Environ. Sci. Technol.* **33,** 1675–1681.

Vance G. F. and David M. B. (1991) Chemical characteristics and acidity of soluble organic substances from a northern hardwood forest floor, central Maine, USA. *Geochim. Cosmochim. Acta* **55,** 3611–3625.

Varadachari C., Mondal A. H., and Ghosh K. (1991) Some aspects of clay-humus complexation: Effect of exchangeable cations and layer charge. *Soil Sci.* **151,** 220–227.

Varadachari C., Mondal A H., Nayak D. C., and Ghosh K. (1994) Clay-humus complexation: Effect of pH and the nature of bonding. *Soil Biol. Biochem.* **26,** 1145–1149.

Varadachari C., Chattopadhyay T., and Ghosh K. (1997) Complexation of humic substances with oxides of iron and aluminum. *Soil Sci.* **162,** 28–34.

Wang L., Chin Y-.P., and Traina, S. J. (1997) Adsorption of (poly) maleic acid and an aquatic fulvic acid by goethite. *Geochim. Cosmochim. Acta* **61,** 5313–5324.

Wershaw R. L., Leenheer J. A., Kennedy K. R., and Noyes T. I. (1996) Use of 13C NMR and FTIR for elucidation of degradation pathways during natural litter decomposition and composting. I. Early stage leaf degradation. *Soil Sci.* **161,** 667–679.

Zinder B., Furrer G., and Stumm W. (1986) The coordination chemistry of weathering. II. Dissolution of Fe(III) oxides. *Geochim. Cosmochim. Acta* **50,** 1861–1869.